NASA Contractor Report 189580

# Fluctuation Diagrams for Hot-Wire Anemometry in Subsonic Compressible Flows

P.C. Stainback
Research Engineer
Analytical Services & Materials Inc.
Hampton, VA 23666

Contract NAS1-19320

K.A. Nagabushana
Research Engineer
Vigyan Inc.
Hampton, VA 23666

Contract NAS1-18585

December 1991

National Aeronautics and
Space Administration

**Langley Research Center**
Hampton, Virginia 23665-5225

**CONTENTS**

## LIST OF FIGURES

**ABSTRACT**

The concept of using "fluctuation diagrams" for describing basic fluctuations in compressible flows was reported by Kovasznay in the 1950's. The application of this technique, for the most part, was restricted to supersonic flows. Recently, Zinov'ev and Lebiga published reports where they considered the fluctuation diagrams in subsonic compressible flows. For the above studies, the velocity and density sensitivities of the heated wires were equal. However, there are considerable data, much taken in the 1950's, which indicate that under some conditions the velocity and density sensitivities are not equal in subsonic compressible flows. Therefore, the present report will describe possible fluctuation diagrams for the cases where the velocity and density sensitivities are equal and the more general case where they are unequal.

## SYMBOLS

$c_p$ specific heat at constant pressure

$c_v$ specific heat at constant volume

$e'$ fluctuating voltage across sensor

$E$ mean voltage across sensor

$\ell$ characteristic length

$M$ Mach number

$m$ mass flow

$p$ pressure

$q$ sensitivity ratio $= \dfrac{S_u}{S_{T_o}}$

$$R_{mT_o} = \frac{\overline{m' T_o'}}{\tilde{m}\ \tilde{T}_o}$$

$$R_{pT_\infty} = \frac{\overline{p' T_\infty'}}{\tilde{p}\ \tilde{T}_\infty}$$

$$R_{u\rho} = \frac{\overline{u' \rho'}}{\tilde{u}\ \tilde{\rho}}$$

$$R_{uT_o} = \frac{\overline{u' T_o'}}{\tilde{u}\ \tilde{T}_o}$$

$$R_{\rho T_o} = \frac{\overline{\rho' T_o'}}{\tilde{\rho}\ \tilde{T}_o}$$

$r$ sensitivity ratio $= \dfrac{S_m}{S_{T_o}}$

$s$ sensitivity ratio $= \dfrac{S_\rho}{S_{T_o}}$

$S_u$ velocity sensitivity

$S_\rho$ density sensitivity

$S_{T_o}$ total temperature sensitivity

$S_m$ mass flow sensitivity

$T_o$ total temperature

$T_\infty$ static temperature

$u$ velocity

$u_s$ source velocity of sound in supersonic flow

$\alpha = \dfrac{1}{(1+\frac{\gamma-1}{2} M^2)}$

$\beta = \alpha(\gamma-1)M$

$\rho$ density

$\gamma$ specific heat ratio = $\dfrac{c_p}{c_v}$

$\theta$ angle between plane wave and axis of probe which is aligned with the flow

$\phi'$ normalized fluctuation voltage ratio = $\dfrac{\frac{e'}{E}}{S_{T_o}}$

$\lambda$ wave length

**Superscripts**

| | |
|---|---|
| $'$ | instantaneous values |
| $\sim$ | RMS values |
| $\overline{\quad}$ | mean values |

**Subscripts**

| | |
|---|---|
| $\omega$ | vorticity |
| $\sigma$ | entropy |
| sf | far-field sound |
| sn | near-field sound |

## INTRODUCTION

The extension of hot wire anemometry to compressible flows was described by Kovasznay[1] in 1950. The concept of "fluctuation diagrams" for describing the basic fluctuations in compressible flows was reported by Kovasznay[2] in 1953, where he showed the existence of three independent modes consisting of vorticity, entropy, and sound. In these two references, the application of the technique, for the most part, was restricted to supersonic flows where the velocity and density sensitivities of the heated wires were equal. In addition to the fluctuation diagrams, Kovasznay also considered cases where only one mode existed thereby generating the so called mode diagrams.

The fluctuation diagrams are graphical representation of the combined fluctuations in a flow determined from hot wire anemometer measurement. The fluctuation diagram can be used to determine the level of fluctuation existing in a flow. For supersonic flows the asymptote of the fluctuation diagram represent the mass flow fluctuation and the intercept on the ordinate represent the total temperature fluctuation. The mode diagram is a special case of the fluctuation diagram where only a given mode is assumed to exist. The consideration of single modes can be often used to identify the predominant mode existing in a flow[3].

Recently Zinov'ev and Lebiga[4,5] published reports where they considered the fluctuation diagrams in subsonic compressible flows where the velocity and density sensitivities were equal. There is, however, a considerable amount of data which

show that under some conditions the velocity and density sensitivities are not equal in subsonic flows[6-9]. Therefore, in the present report the fluctuation diagrams and mode diagrams will be considered for the cases where the velocity and density sensitivities are equal and for cases where they are unequal.

## RESULTS

### VELOCITY AND DENSITY SENSITIVITIES EQUAL

#### Fluctuation Diagram

In supersonic flows it has been shown that, from experimental results, the velocity and density sensitivities are equal. For the test conditions of references 4 and 5 this equality was also found to be true for subsonic compressible flows. Under these conditions, the heat transfer from a heated wire is a function of mass flow and total temperature and the following equation is applicable for a constant current anemometer (CCA)[1]:

$$\frac{e'}{E} = - S_m \frac{m'}{m} + S_{T_o} \frac{T_o'}{T_o} \qquad (1)$$

Dividing equation 1 by the total temperature sensitivity, squaring, then taking the mean, results in the following:

$$\overline{\phi'^2} = r^2 \overline{\left(\frac{m'}{m}\right)^2} + \overline{\left(\frac{T_o'}{T_o}\right)^2} - 2rR_{mT_o} \left(\frac{\tilde{m}}{m}\right) \left(\frac{\tilde{T}_o}{T_o}\right) \qquad (2)$$

This equation was obtained by Kovasznay and was used to generate fluctuation diagrams for supersonic flows. This equation was also used in references 4 and 5 for subsonic compressible flows.

The general form of equation 2 represents a hyperbola where the intercept on the $\phi$ axis represents the total temperature fluctuation and the asymptotes represent the mass flow fluctuation[10].

## Mode Diagrams

Kovasznay[2] demonstrated that fluctuations in compressible flows are composed of three independent "modes" for small fluctuations. These modes consist of vorticity (velocity fluctuations), entropy (static temperature fluctuations), and sound (pressure fluctuations).

For the case of subsonic flows with a single mode, equation 1 was used in Appendix A to obtain equation for the mode diagrams. The mode diagrams for vorticity and entropy are identical for subsonic and supersonic speeds (see equations A-3 and A-5).

When considering the sound mode, there are two possibilities for subsonic flows. The sound can be of the far or near-field type. The sound field can be considered to be of the far-field type if $\lambda/\ell \ll 1$. For near-field sound the quantity $\lambda/\ell \approx 1$. The relationship between pressure and velocity for the far-field sound is given by the plane wave equation as[3]:

$$\frac{u'}{u} = \frac{1}{\gamma M}\left(\frac{p'}{p}\right)_{sf} \cos\theta \qquad (3)$$

For near-field sound, the relationship between pressure and velocity can be obtained from the compressible Bernoulli's equation as:

$$\frac{u'}{u} = -\frac{1}{\gamma M^2}\left(\frac{p'}{p}\right)_{sn}\cos\theta \qquad (4)$$

For far-field sound, the equation for the mode diagram is derived in Appendix A and is given by equation A-7. The equation for the mode diagram is identical to the one for supersonic flow. However, for subsonic flow the value of $\cos\theta$ can range between -1 and 1. In supersonic flow, for stationary Mach waves, the $\cos\theta = -\frac{1}{M}$. The value of the $\cos\theta$ for moving sources of sound is[3]:

$$\cos\theta = -\frac{1}{M\left(1 - \frac{u_s}{u}\right)} \qquad (5)$$

An example of far-field sound for subsonic flow is presented in Figure 1 for $\left(\frac{\tilde{p}}{p}\right)_{sf} = 0.01$ and $M = 0.50$. The only case for subsonic flow which is similar to the case for supersonic flow occurs for $\theta = 180^{\circ}$, ie. upstream moving sound. In the test section of supersonic tunnels the dominant disturbance is also upstream moving sound relative to the flow velocity[3].

Near-field sound is often not considered for supersonic flow. However, because of the low frequencies existing in

subsonic flows, there is a high probability that much of the sound in low speed wind tunnels is due to near-field sound.

The equation for the fluctuation diagram for near-field sound in subsonic flow was derived in Appendix A by substituting Bernoulli's equation along with the equation of state and the energy equation into equation 1 to give equation A-9. Equation A-9 shows that there is not a single fluctuating quantity for near-field sound since the fluctuation diagram is made up of a pressure term and a static temperature term and their correlation. For various values of $\tilde{p}$, $\tilde{T}$, and $R_{pT_\infty}$, different fluctuation diagrams could be obtained. An example of the fluctuation diagram is presented in Figure 2 for $\left(\frac{\tilde{p}}{p}\right)_{sn}$ = 0.01, $\left(\frac{\tilde{T}_\infty}{T_\infty}\right)_{sn}$ = 0.01, $R_{pT_\infty}$ = 1 and M = 0.50. This fluctuation diagram, where it is assumed that $R_{pT_\infty}$ = 1, is significantly different from the ones obtained for far-field sound. For $\theta$ = 90° there are no mass flow fluctuations.

## Multi-mode Fluctuation Diagrams

In general, more than one mode would be expected to exist in a given flow. Equation 1 was used in Appendix A to obtain fluctuation diagrams for multi-modes. First consider the case where vorticity, entropy, and near-field sound coexist in a flow but are uncorrelated, and the correlation between pressure and static temperature for near-field sound is assumed to be 1. The equation describing this situation is

given by equation A-11. An example of the fluctuation diagram for these fluctuations is presented in Figure 3.

The equation describing the combined effects of vorticity and entropy is derived in Appendix A and is given by equation A-12. An example of this fluctuation diagram is presented in figure 4 for $\left(\frac{\tilde{u}}{u}\right)_{\omega} = 0.01$, $\left(\frac{\tilde{T}_{\infty}}{T_{\infty}}\right)_{\sigma} = 0.01$, and M=0.50. The combined effect of vorticity and entropy fluctuations for subsonic flow is identical to the one for supersonic flow and has been described by Kovasznay[2].

Another highly probable combination of fluctuations is vorticity and near-field sound. An equation describing this situation was derived in Appendix A (Equation A-13). An example of these two types of fluctuations is presented in Figure 5. This fluctuation diagram is similar to the one obtained for the combined effects of vorticity, entropy, and near-field sound as shown in figure 3.

## VELOCITY AND DENSITY SENSITIVITIES NOT EQUAL

### Fluctuation Diagrams

Data were presented in references 8 and 9 which indicate that under some conditions the velocity and density sensitivities were not equal in subsonic flows, (Mach number as low as 0.05 and slip flow conditions) and in transonic flows. These data are in agreement with earlier results presented in references 6 and 7.

In the present study, mode or fluctuation diagrams will be presented for subsonic flows where the velocity and density sensitivities are considered to be different. The following equation is applicable for constant current anemometers (CCA) in compressible flows[11]:

$$\frac{e'}{E} = - S_u \frac{u'}{u} - S_\rho \frac{\rho'}{\rho} + S_{T_o} \frac{T_o'}{T_o} \qquad (6)$$

Squaring equation 6, forming the mean, and dividing by $S_{T_o}^2$ gives:

$$\overline{\phi'^2} = q^2 \overline{\left(\frac{u'}{u}\right)^2} + s^2 \overline{\left(\frac{\rho'}{\rho}\right)^2} + \overline{\left[\frac{T_o'}{T_o}\right]^2} + 2\, q\, s\, R_{u\rho} \frac{\tilde{u}}{u} \frac{\tilde{\rho}}{\rho}$$

$$- 2\, q\, R_{uT_o} \frac{\tilde{u}}{u} \frac{\tilde{T}_o}{T_o} - 2\, s\, R_{\rho T_o} \frac{\tilde{\rho}}{\rho} \frac{\tilde{T}_o}{T_o} \qquad (7)$$

This is the general equation for a wire mounted normal to the flow in compressible flows where $S_u \neq S_\rho$. This is a single equation with six unknowns. In principal, this equation can be solved by operating a single wire at six overheats and solving six equations to obtain the three fluctuating quantities and their correlations. In the past it was generally stated that the calibration of the wire cannot be made sufficiently accurate or the velocity and density sensitivities cannot be made sufficiently different to obtain a suitable solution using this technique. Recently a three wire technique[8,9] was used to make measurements based on an equation similar to equation 6 but applicable for a constant

temperature anemometer (CTA). These results indicated that under some conditions the density sensitivity could be two to three times greater than the velocity sensitivity. Under these conditions it should be possible to use a CCA operated at many overheats to obtain solutions to equation 7 using a multiple linear regression technique. The results obtained using the three wire probe technique with a CTA and a single wire probe with a CCA could be compared to determine the possible accuracy of the two systems.

The major difficulty in making these measurements using the multi-wire technique of references 8 and 9 is making the velocity and the density sensitivities sufficiently different for the three wires. The major difficulty of using a CCA and equation 7 to obtain the three fluctuations and their correlations would be to insure that the velocity and density sensitivities are sufficiently different over the range of overheats so that the sensitivity matrix for equation 7 is well conditioned.

Assuming that the velocity and density sensitivities are sufficiently different so that solutions for equation 7 are possible, what are the characteristics of the fluctuation diagrams? In equation 7, $\phi$ is a function of q and s, therefore, the fluctuation diagram exists on a three-dimensional surface, a hyperboloid, rather than a plane as for the case when $S_u = S_\rho$. However, the important information exists in the $\phi$-q and $\phi$-s planes. For example when s = 0, equation 7 reduces to an equation for a hyperbola in the $\phi$-q plane where the asymptote gives the velocity fluctuations. If q = 0, again equation 7 reduces to an equation for a hyperbola in

the $\phi$-s plane and the asymptote represents the density fluctuations. When q and s are zero, the intercept on the $\phi$ axis gives the fluctuations for the total temperature. In planes parallel to the q-s plane, the locus of points of the fluctuation diagram is governed by the velocity and density fluctuations and their correlation. The cross product term, qs, requires a rotation of the axis before the characteristics of the locus can be identified. For example, if it is assumed that $\frac{\tilde{u}}{u} = 0.01$, $\frac{\tilde{\rho}}{\rho} = 0.005$, $\frac{\tilde{T}_o}{T_o} = 0.001$, $R_{u\rho} = -0.8$, $R_{uT_o} = -0.6$ and $R_{\rho T_o} = 0.5$, the locus of the points in planes parallel to the q-s plane are ellipses rotated $66.6^\circ$ from the q axis. The locus of points of the fluctuation diagram on the surface of the hyperboloid will depend on the relative changes in q and s as the overheat of the wire is changed.

Although the fluctuation diagram exists on the surface of a hyperboloid, the fluctuations can be determined from the intersection of the hyperboloid with the $\phi$-q and $\phi$-s planes. Because of this the fluctuation and mode diagrams will be defined as the traces of these intersections in the noted planes. A general schematic representation of the fluctuation diagram for equation 7 is presented in figure 6. Work along this line was considered by research personnel at Novosibirsk, USSR. However, for their flow conditions $S_u$ was apparently equal to $S_\rho$ and the more general solution was not required[12].

If it is assumed that q = s, equation 7 reduces to the conventional equation for supersonic flow. Therefore, the mode diagram for supersonic flow lies in the $\phi$-r plane which

lies between the $\phi$-q and $\phi$-s planes. A sketch of this situation is presented in figure 7.

**Mode Diagrams**

If it is assumed that the fluctuations are only vorticity, it is shown in Appendix B that equation 7 reduces to equation B-3. Results obtained using this equation for the case where $\left(\frac{\tilde{u}}{u}\right)_\omega = 0.01$ are presented in Figure 8. The mode diagram for vorticity is identical to the one for supersonic flows except that $S_m$ is replaced by $S_u$ in the equation. The mode diagram lies in the $\phi$-q plane. Equation B-3 shows that when $\phi = 0$ then $q = \beta$. Also, when $q = 0$ then:

$$\tilde{\phi} = \beta \left(\frac{\tilde{u}}{u}\right)_\omega \qquad (8)$$

which represents the total temperature fluctuation due to vorticity.

Next assume that the fluctuations are all entropy. Then equation 7, as shown in Appendix B, reduces to equation B-4. Equation B-4 is identical to the one for supersonic flow except that $S_m$ is replaced by $S_\rho$ and the mode diagram lies in the $\phi$-s plane.

An example of the mode diagram for entropy when $\left(\frac{\tilde{T}_\infty}{T_\infty}\right)_\sigma = 0.01$ is presented in figure 9. Here again, only the

$\phi$-s plane is presented. When $\phi = 0$ then $s = -\alpha$, and when $s = 0$ then:

$$\tilde{\phi} = \alpha \left(\frac{\tilde{T}_\infty}{T_\infty}\right)_\sigma \qquad (9)$$

which represent the total temperature fluctuation due to entropy fluctuations.

Now assume that all the fluctuations are far-field sound (that is $\lambda/\ell << 1$). The equation (B-5) for this case is derived in Appendix B. Equation B-5 represents a three dimensional surface in the $\phi$, q, s coordinate system and the mode diagram lies on this surface. The intersection of the surface in the $\phi$-q and $\phi$-s planes are given by equations B-6 and B-7, respectively. In this report these intersections are defined as the mode diagrams.

An example of the sound mode for the far-field is presented in figure 10. Note that the $\phi$-s plane has been rotated into the plane of the paper. Figure 1 and 10 show that there is a significant difference between the mode diagrams for far-field sound for the cases where $S_u = S_\rho$ and for the case where $S_u \neq S_\rho$.

Near-field sound can be considered to be either incompressible or compressible. From Appendix B the equation for near-field sound for compressible flow is given by equation B-14. As for the case where $S_u = S_\rho$, this equation consist of pressure and temperature terms and their correlation. For s =

0 and q = 0, equation B-14 reduces to equations B-15 and B-16, respectively.

An example of this type of fluctuation diagram is presented in figure 11. Again the $\phi$-s plane has been rotated into the plane of the paper. This result is again not general since different assumptions about the fluctuation levels and their correlations would result in different fluctuation diagrams.

In subsonic flow it is possible for sound to enter the test section from any direction since $\cos\theta$ can range from -1 to 1, and it is probable that more than one source can contribute to the sound field in the test section. The sound mode is further complicated by the possible existence of near and far-field sound sources whose effect in the test section is a function of frequency. In addition, the sound can be reflected, refracted, and diffracted in the wind tunnel circuit in a manner which depends on the geometry of the tunnel and the characteristics of the sound.

Because of these problems which make the sound mode extremely complicated, it is doubtful that a single sound mode would be observed in subsonic wind tunnels unless it was introduced artificially. The correct analysis of the characteristics of sound would probably require measurements using multiple sensors and various data reduction methods based on cross correlation techniques.

## Multi-mode Fluctuation Diagrams

The existence of more than one mode can also be considered for the case where $S_u \neq S_\rho$. First consider the case where the fluctuations consist of vorticity, entropy, and near-field sound where the fluctuations are assumed to be uncorrelated. The equation for this case is derived in Appendix B and is given by equation B-17.

When s = 0 and q = 0, equation B-17 reduces to equations B-18 and B-19, respectively. An example of this fluctuation diagram is presented in Figure 12 for the case where $\left(\frac{\tilde{u}}{u}\right)_\omega$, $\left(\frac{\tilde{T}_\infty}{T_\infty}\right)_\sigma$, $\left(\frac{\tilde{p}}{p}\right)_{sn}$, $\left(\frac{\tilde{T}_\infty}{T_\infty}\right)_{sn} = 0.01$, $R_u\left(T_\infty\right)_\sigma = 1$, and M = 0.50. This figure shows that, for these assumptions, the fluctuation diagram in the $\phi$-q plane for $\theta = 0$ and $180^\circ$ are identical. Also, there is very little difference between the fluctuation diagrams in the $\phi$-s planes for the values of $\theta$ assumed.

Equation B-21 shown in Appendix B illustrates the case where vorticity and entropy coexist. If s = 0 and q = 0, equation B-21 reduces to equations B-22 and B-23, respectively. An example of the fluctuation diagram for this case is shown in Figure 13 for $\left(\frac{\tilde{u}}{u}\right)_\omega$, $\left(\frac{\tilde{T}_\infty}{T_\infty}\right)_\sigma = 0.01$, $R_{uT_\infty} = 1$, and M = 0.50.

Finally consider the case where vorticity and near-field sound coexist and there is no correlation between the fluctuations. The equation for this situation is derived in

Appendix B and is given by equation B-25. For s = 0 and q = 0, equation B-25 reduces to equations B-26 and B-27, respectively. An example of this type of combined fluctuation is shown in Figure 14 for $\left(\frac{\tilde{u}}{u}\right)_{\omega}$, $\left(\frac{\tilde{T}_{\infty}}{T_{\infty}}\right)_{sn}$, $\left(\frac{\tilde{p}}{p}\right)_{sn} = 0.01$, $R_{up} = 0$, $R_{pT_{\infty}} = 1$, and M = 0.50. For the conditions assumed, there are no density fluctuations. This result, however, depends on the conditions assumed for the fluctuation levels and their correlations.

Very little experimental data are available in the literature describing the mode diagrams for subsonic compressible flows. A limited amount of data were presented in references 4 and 5 for a case where sound was artificially introduced into the test section and dominated the disturbance levels. Vorticity and entropy were also artificially introduced into the test section where it was assumed that their levels were about the same and the sound level was small. For these cases it was determined that $S_u = S_{\rho}$. Examples of fluctuation diagrams obtained from ref. 4 are presented in figure 15. The data shown in figure 15-a were obtained when sound was introduced into the test section upstream of the hot wire probe. This fluctuation diagram agrees in shape with the results presented in figure 1 for far-field sound with $\theta = 0$, i.e., down stream moving sound.

The results presented in figure 15-b, for the case where vorticity and entropy dominated the flow, is similar to the results presented in figure 4 for $R_{mT_{\infty}}$ between 1 and 0. This similarity would be improved by using the correct Mach

number and selecting various values for $\tilde{u}$, $\tilde{T}_\infty$, and $R_{mT_\infty}$ in equation A-12.

## CONCLUDING REMARKS

The present paper extends the fluctuation diagrams developed by Kovasznay for supersonic flows to subsonic compressible flows where $S_u = S_\rho$ and to the more general case where $S_u \neq S_\rho$. The fluctuation and mode diagrams developed by Kovasznay were limited to supersonic flows where the velocity and density sensitivities of the sensor were equal. For this case and for subsonic flow where $S_u = S_\rho$, the fluctuation diagrams could be pictured as existing in a plane. In subsonic slip and transonic flows, where the velocity and density sensitivities can be different, it was shown that the fluctuation diagrams could be pictured as existing on a three-dimensional surface in the $\phi$, q, s coordinate system. However, the important information would exist in the $\phi$-q and $\phi$-s planes. For this case, the fluctuation diagrams were significantly different from those in supersonic flow and in subsonic flow where $S_u = S_\rho$. This was particularly true for the sound mode.

When $S_u = S_\rho$ for subsonic flow, the vorticity and entropy mode diagrams were identical to those for supersonic flow. However the sound "modes" could be significantly different from those for supersonic flows.

For cases where the velocity and density sensitivities are sufficiently different to permit the calculation of the velocity, density, and total temperature fluctuations, the fluctuation diagrams and mode diagrams should be useful for identifying the dominant mode existing in subsonic slip or transonic flows.

## REFERENCES


1. Kovasznay, L.S.G., 1950, "The Hot-Wire Anemometer in Supersonic Flows," Journal of the Aeronautical Sciences, Vol 17, No. 9, pp 565-584.

2. Kovasznay, L.S.G., 1953, "Turbulence in Supersonic Flow," Journal of the Aeronautical Sciences, Vol 20, No. 10, pp 657-674.

3. Laufer, J., 1961, "Aerodynamic Noise in Supersonic Wind Tunnels," Journal of the Aerospace Sciences, pp 685-692.

4. Zinov'ev, V.N., and Lebiga, V.A., 1988, "Measurements of Fluctuations For High Subsonic Velocities Using a Hot-Wire Anemometer," Plenum Publishing Corp 1988 Novosibirsk, Translated from Zhurnal Prikladoni Mekhaniki i Teckhnicheskoi Fiziki, No. 3, pp 80-84.

5. Lebiga, V.A., and Zinoviev, V.N., 1989, "Hot-Wire Measurements in Compressible Flow," Institute of Theoretical and Applied Mechanics, Novosibirsk, USSR.

6. Spangenberg, W.G., 1955, "Heat Loss Characteristics of Hot-Wire Anemometers at Various Densities in Transonic and Supersonic Flows," NACA TN 3381.

7. Baldwin, L.V., 1958, "Slip-Flow Heat Transfer From Cylinders in Subsonic Airstreams," NACA TN 4369.

8. Jones,G.S., and Stainback,P.C., 1988, "A New Look at Wind Tunnel Flow Quality for Transonic Flows," SAE 881452 Aerospace Technology Conference and Exposition, Anaheim, California.

9. Stainback, P.C., Nagabushana, K.A., Clukey, S.J., and Jones, G.S., 1991, "Heat Transfer From Heater Cylinders in Subsonic Flows," First Joint ASME-JSME Fluids Engineering Conference, Portland, Oregon, June 23-26.

10. Anders, John B.,Jr, 1974, "Turbulence Measurements in Hypersonic Helium Flow," Report 1157, Gas Dynamics Laboratory, Princeton University, Princeton, New Jersey.

11. Morkovin, M.V., 1956, "Fluctuations and Hot Wire Anemometry in Compressible Flows," AGARDograph 24.

12. Lebiga, V.A., 1991, Private communication

## APPENDIX A

### CASES FOR WHICH THE VELOCITY AND DENSITY SENSITIVITIES ARE EQUAL

If $S_u = S_\rho$ then the equation for a CCA is:

$$\frac{e'}{E} = - S_m \frac{m'}{m} + S_{T_o} \frac{T_o'}{T_o} \qquad \text{A-1}$$

Assuming that the only fluctuation is vorticity gives:

$$\frac{m'}{m} = \frac{u'}{u} + \frac{\rho'}{\rho} \qquad \text{A-2}$$

$$\frac{u'}{u} = \left(\frac{u'}{u}\right)_\omega \; ; \qquad \frac{\rho'}{\rho} = 0; \qquad \frac{T_o'}{T_o} = \beta \left(\frac{u'}{u}\right)_\omega$$

Substituting the above equations into equation A-1, dividing by $S_{T_o}$, squaring, and taking the mean gives:

$$\overline{\phi'^2} = (\beta - r)^2 \overline{\left(\frac{u'}{u}\right)_\omega^2} \qquad \text{A-3}$$

This equation is identical to the one obtained for supersonic flow.

Next, assume that all the fluctuations are entropy, then:

$$\frac{u'}{u} = 0 \; ; \; \frac{\rho'}{\rho} = -\left(\frac{T'_\infty}{T_\infty}\right)_\sigma \; ; \; \frac{T'_o}{T_o} = \alpha \left(\frac{T'_\infty}{T_\infty}\right)_\sigma ;$$

A-4

$$\frac{m'}{m} = -\left(\frac{T'_\infty}{T_\infty}\right)_\sigma$$

Substituting the above equations into equation A-1 gives:

$$\overline{\phi'^2} = (r + \alpha)^2 \overline{\left(\frac{T'_\infty}{T_\infty}\right)_\sigma^2} \qquad \text{A-5}$$

Next assume that all the fluctuations are far-field sound. Then:

$$\frac{u'}{u} = \frac{1}{\gamma M}\left(\frac{p'}{p}\right)_{sf} \cos\theta \; ; \; \frac{\rho'}{\rho} = \frac{1}{\gamma}\left(\frac{p'}{p}\right)_{sf} ; \; \frac{T'_\infty}{T_\infty} = \frac{(\gamma-1)}{\gamma}\left(\frac{p'}{p}\right)_{sf}$$

A-6

$$\frac{T'_o}{T_o} = \alpha \frac{(\gamma-1)}{\gamma}\left(\frac{p'}{p}\right)_{sf} + \beta\left(\frac{u'}{u}\right)_{sf} ; \; \frac{m'}{m} = \frac{1}{\gamma M}\left(\frac{p'}{p}\right)_{sf} \cos\theta + \frac{1}{\gamma}\left(\frac{p'}{p}\right)_{sf}$$

Substituting the above equations into equation A-1, dividing by $S_{T_o}$, squaring, and taking the mean gives:

$$\overline{\phi'^2} = [\alpha(\gamma-1)M + \beta\cos\theta - r(\cos\theta + M)]^2 \frac{1}{\gamma^2 M^2} \overline{\left(\frac{p'}{p}\right)_{sf}^2} \qquad \text{A-7}$$

Assuming near-field sound gives:

$$\frac{u'}{u} = -\frac{1}{\gamma M^2}\left(\frac{p'}{p}\right)_{sn}\cos\theta\,; \quad \frac{\rho'}{\rho} = \left(\frac{p'}{p}\right)_{sn} - \left(\frac{T'_\infty}{T_\infty}\right)_{sn}$$

$$\frac{m'}{m} = \left(\frac{p'}{p}\right)_{sn} - \left(\frac{T'_\infty}{T_\infty}\right)_{sn} - \frac{1}{\gamma M^2}\left(\frac{p'}{p}\right)_{sn}\cos\theta \qquad \text{A-8}$$

$$\frac{T'_o}{T_o} = \alpha\left(\frac{T'_\infty}{T_\infty}\right)_{sn} - \beta\,\frac{1}{\gamma M^2}\left(\frac{p'}{p}\right)_{sn}\cos\theta$$

Substituting the above equations into equation A-1, dividing by $S_{T_o}$, squaring, and taking the mean gives:

$$\overline{\phi'^2} = [(r-\beta)\cos\theta - \gamma M^2]^2\,\frac{1}{\gamma^2 M^4}\,\overline{\left(\frac{p'}{p}\right)^2_{sn}} +$$

$$(r+\alpha)^2\,\overline{\left(\frac{T'_\infty}{T_\infty}\right)^2_{sn}} + \qquad \text{A-9}$$

$$2(r+\alpha)[r(\cos\theta - \gamma M^2) - \beta\cos\theta]\,\frac{1}{\gamma M^2}\,R_{pT_\infty}\left(\frac{\tilde{T}_\infty}{T_\infty}\right)_{sn}\left(\frac{\tilde{p}}{p}\right)_{sn}$$

Next consider the case where more than one mode exist in the flow. First consider the existence of vorticity, entropy, and near-field sound where it is assumed that there is no correlation between the modes:

$$\frac{u'}{u} = \left(\frac{u'}{u}\right)_\omega - \frac{1}{\gamma M^2}\left(\frac{p'}{p}\right)_{sn}\cos\theta$$

$$\frac{\rho'}{\rho} = -\left(\frac{T'_\infty}{T_\infty}\right)_\sigma + \left(\frac{p'}{p}\right)_{sn} - \left(\frac{T'_\infty}{T_\infty}\right)_{sn} \qquad \text{A-10}$$

$$\frac{m'}{m} = \left(\frac{u'}{u}\right)_\omega - \frac{1}{\gamma M^2}\left(\frac{p'}{p}\right)_{sn}\cos\theta - \left(\frac{T'_\infty}{T_\infty}\right)_\sigma + \left(\frac{p'}{p}\right)_{sn} - \left(\frac{T'_\infty}{T_\infty}\right)_{sn}$$

$$\frac{T'_o}{T_o} = \beta\left(\frac{u'}{u}\right)_\omega - \beta\frac{1}{\gamma M^2}\left(\frac{p'}{p}\right)_{sn}\cos\theta + \alpha\left\{\left(\frac{T'_\infty}{T_\infty}\right)_\sigma + \left(\frac{T'_\infty}{T_\infty}\right)_{sn}\right\}$$

Substituting the above equations into equation A-1 , dividing by $S_{T_o}$, squaring, and taking the mean gives:

$$\overline{\phi'^2} = (\beta - r)^2\overline{\left(\frac{u'}{u}\right)^2_\omega} + [r(\gamma M^2 - \cos\theta)+\beta]^2\frac{1}{\gamma^2 M^4}\overline{\left(\frac{p'}{p}\right)^2_{sn}} +$$

$$(r+\alpha)^2\left[\overline{\left(\frac{T'_\infty}{T_\infty}\right)^2_\sigma} + \overline{\left(\frac{T'_\infty}{T_\infty}\right)^2_{sn}}\right] - \qquad \text{A-11}$$

$$2\,[r(\gamma M^2 - \cos\theta) + \beta](r + \alpha)\frac{1}{\gamma M^2}R_{pT_\infty}\left(\frac{\tilde{p}}{p}\right)_{sn}\left(\frac{\tilde{T}_\infty}{T_\infty}\right)_{sn}$$

Next consider the combined effects of vorticity and entropy. Substituting equations A-2 and A-4 into A-1 gives:

$$\overline{\phi'^2} = (\beta-r)^2\overline{\left(\frac{u'}{u}\right)^2}_{\omega} + (\alpha+r)^2\overline{\left(\frac{T'_\infty}{T_\infty}\right)^2}_{\sigma} + 2(\beta-r)(\alpha+r)R_{uT_\infty}\left(\frac{\tilde{u}}{u}\right)_{\omega}\left(\frac{\tilde{T}_\infty}{T_\infty}\right) \qquad \text{A-12}$$

Finally consider the combined effects of vorticity and near-field sound where it is assumed that there is no correlation between the fluctuations:

$$\overline{\phi'^2} = (\beta-r)^2\overline{\left(\frac{u'}{u}\right)^2}_{\omega} + (r+\alpha)^2\overline{\left(\frac{T'_\infty}{T_\infty}\right)^2}_{sn} + [r(\gamma M^2-\cos\theta)+\beta]^2\frac{1}{\gamma^2M^4}\overline{\left(\frac{p'}{p}\right)^2}_{sn}$$

$$-2[r(\gamma M^2-\cos\theta)+\beta](r+\alpha)\frac{1}{\gamma M^2}R_{pT_\infty}\left(\frac{\tilde{p}}{p}\right)_{sn}\left(\frac{\tilde{T}_\infty}{T_\infty}\right)_{sn} \qquad \text{A-13}$$

## APPENDIX B

### EQUATIONS FOR MODE DIAGRAMS IN SUBSONIC COMPRESSIBLE FLOWS FOR CASES WHERE $S_u \neq S_\rho$

For compressible flows the following equation was presented in reference 11 for a constant current anemometer:

$$\frac{e'}{E} = - S_u \frac{u'}{u} - S_\rho \frac{\rho'}{\rho} + S_{T_o} \frac{T_o'}{T_o} \qquad \text{B-1}$$

Squaring equation B-1, dividing by $S_{T_o}$, and taking the mean gives:

$$\overline{\phi'^2} = q^2 \overline{\left(\frac{u'}{u}\right)^2} + s^2 \overline{\left(\frac{\rho'}{\rho}\right)^2} + \overline{\left(\frac{T_o'}{T_o}\right)^2} + 2 q s R_{u\rho} \frac{\tilde{u}}{u} \frac{\tilde{\rho}}{\rho} -$$

$$2 q R_{uT_o} \frac{\tilde{u}}{u} \frac{\tilde{T}_o}{T_o} - 2 s R_{\rho T_o} \frac{\tilde{\rho}}{\rho} \frac{\tilde{T}_o}{T_o} \qquad \text{B-2}$$

Equation B-2 is the general equation that relates the voltage fluctuation across a heated wire to fluctuations of the flow variables.

Assuming that all the fluctuations are due to vorticity and using equation A-2 and B-1 gives:

$$\overline{\phi'^2} = \overline{\left(\frac{u'}{u}\right)^2}_{\omega} (q - \beta)^2 \qquad \text{B-3}$$

The vorticity mode is represented by straight lines, one of which has a negative slope for values of q between 0 and $\beta$. The other line has a positive slope for q greater than $\beta$.

Assume that all the fluctuations are due to entropy, and using equation A-4 and B-1 gives:

$$\overline{\phi'^2} = \overline{\left(\frac{T'_\infty}{T_\infty}\right)^2}_{\sigma} (s + \alpha)^2 \qquad \text{B-4}$$

There are two possible solutions for the sound mode: far-field sound and near-field sound. First consider that all of the fluctuations are of the far-field type, then substituting equation A-6 into B-1 gives:

$$\overline{\phi'^2} = \frac{1}{\gamma^2 M^2} \overline{\left(\frac{p'}{p}\right)^2}_{sf} \{(\beta - q) \cos\theta + [\alpha(\gamma - 1) - s] M\}^2 \qquad \text{B-5}$$

If s = 0 then:

$$\overline{\phi'^2} = \frac{1}{\gamma^2 M^2} \overline{\left(\frac{p'}{p}\right)^2}_{sf} \{(\beta - q) \cos\theta + \alpha(\gamma - 1) M\}^2 \qquad \text{B-6}$$

If $\phi$ = 0 then:

$$q = \frac{\alpha(\gamma - 1)M}{\cos\theta} + \beta \qquad \text{B-7}$$

and if q = 0 then:

$$\overline{\phi'^2} = \frac{1}{\gamma^2 M^2} \overline{\left(\frac{p'}{p}\right)}^2_{sf} \{\beta \cos\theta + \alpha(\gamma - 1) M\}^2 \qquad \text{B-8}$$

Now assume that q = 0 in equation B-5, then:

$$\overline{\phi'^2} = \frac{1}{\gamma^2 M^2} \overline{\left(\frac{p'}{p}\right)}^2_{sf} \{\beta \cos\theta + [\alpha(\gamma - 1) - s] M\}^2 \qquad \text{B-9}$$

For $\phi = 0$:

$$s = \frac{\beta \cos\theta}{M} + \alpha(\gamma - 1) \qquad \text{B-10}$$

and for s = 0:

$$\overline{\phi'^2} = \frac{1}{\gamma^2 M^2} \overline{\left(\frac{p'}{p}\right)}^2_{sf} \{\beta \cos\theta + \alpha(\gamma - 1) M\}^2 \qquad \text{B-11}$$

Finally, assume that all the fluctuations are of the near-field type. For this assumption the flow can be considered as being either incompressible or compressible. First consider the incompressible case where $\frac{\rho'}{\rho} = 0$. Under these assumptions equation B-1 becomes:

$$\frac{e'}{E} = (\beta\, S_{T_o} - S_u)\, \frac{u'}{u} + \alpha\, S_{T_o}\, \frac{T_\infty'}{T_\infty} \qquad \text{B-12}$$

Using equation A-8 in the equation B-1 with $\frac{\rho'}{\rho} = 0$, dividing by $S_{T_o}$, squaring the equation, and taking the mean gives:

$$\overline{\phi'^2} = \frac{1}{\gamma^2 M^4}\,(q - \beta)^2 \cos^2\theta\, \overline{\left(\frac{p'}{p}\right)^2}_{sn} + \alpha^2\, \overline{\left(\frac{T_\infty'}{T_\infty}\right)^2}_{sn} +$$

$$2\,\frac{\alpha \cos\theta}{\gamma M^2}\,(q - \beta)\, R_{pT_\infty}\left(\frac{\tilde{p}}{p}\right)_{sn}\left(\frac{\tilde{T}_\infty}{T_\infty}\right)_{sn} \qquad \text{B-13}$$

Equation B-13 shows that for near-field sound there are two fluctuating quantities, a pressure term and a temperature term, and their correlation. The fluctuation diagram lies in the $\phi$-q plane for the incompressible flow case.

Next consider near-field sound for compressible flows. Using equation A-8 in the equation B-1, dividing by $S_{T_o}$, squaring the result, and taking the mean gives:

$$\overline{\phi'^2} = \left[\cos\theta\,(q - \beta) - \gamma M^2 s\right]^2 \frac{1}{\gamma^2 M^4}\, \overline{\left(\frac{p'}{p}\right)^2}_{sn} +$$

$$(\alpha + s)^2\, \overline{\left(\frac{T_\infty'}{T_\infty}\right)^2}_{sn} + \qquad \text{B-14}$$

$$2\,(\alpha + s)\left[\cos\theta\,(q - \beta) - \gamma M^2 s\right]\frac{1}{\gamma M^2}\, R_{pT_\infty}\left(\frac{\tilde{p}}{p}\right)_{sn}\left(\frac{\tilde{T}_\infty}{T_\infty}\right)_{sn}$$

Again the near-field sound in compressible flow is made up of two fluctuations and their correlation. The fluctuation diagram lies on a surface in the $\phi$, q, s coordinate system.

If s = 0, equation B-14 becomes

$$\overline{\phi'^2} = \left[\cos\theta\,(q - \beta)\right]^2 \frac{1}{\gamma^2 M^4} \overline{\left(\frac{p'}{p}\right)^2}_{sn} + \alpha^2 \overline{\left(\frac{T'_\infty}{\bar{T}_\infty}\right)^2}_{sn} +$$

$$2\,\alpha \left[\cos\theta\ (q - \beta)\right] \frac{1}{\gamma M^2} R_{pT_\infty} \left(\frac{\tilde{p}}{p}\right)_{sn} \left(\frac{\tilde{T}_\infty}{\bar{T}_\infty}\right)_{sn} \qquad \text{B-15}$$

If q = 0, then equation B-14 becomes

$$\overline{\phi'^2} = \left[\ -\beta\ \cos\theta\ -\gamma M^2 s\right]^2 \frac{1}{\gamma^2 M^4} \overline{\left(\frac{p'}{p}\right)^2}_{sn} + (\alpha + s)^2 \overline{\left(\frac{T'_\infty}{\bar{T}_\infty}\right)^2}_{sn}$$

$$2\ (\alpha + s) \left[\beta\cos\theta + \gamma M^2 s\right] \frac{1}{\gamma M^2} R_{pT_\infty} \left(\frac{\tilde{p}}{p}\right)_{sn} \left(\frac{\tilde{T}_\infty}{\bar{T}_\infty}\right)_{sn} \qquad \text{B-16}$$

For most flow conditions more than one mode will probably be present in the flow. Some of the possible multi-mode conditions will be considered. First consider the coexistence of vorticity, entropy, and near-field sound where they are uncorrelated. Substituting equations A-2, A-4 and A-8 into B-1 gives:

$$\overline{\phi'^2} = (\beta - q)^2 \overline{\left(\frac{u'}{u}\right)^2}_{\omega} + (s + \alpha)^2 \left( \overline{\left(\frac{T'_\infty}{\overline{T}_\infty}\right)^2}_{sn} + \overline{\left(\frac{T'_\infty}{\overline{T}_\infty}\right)^2}_{\sigma} \right) +$$

$$(q - \beta)^2 \frac{1}{\gamma^2 M^4} \overline{\left(\frac{p'}{p}\right)^2}_{sn} \cos^2\theta + \qquad \text{B-17}$$

$$2(s + \alpha)(q - \beta) \frac{1}{\gamma M^2} R_{pT_\infty} \left(\frac{\tilde{T}_\infty}{\overline{T}_\infty}\right)_{sn} \left(\frac{\tilde{p}}{p}\right)_{sn}$$

If s = 0, this equation becomes:

$$\overline{\phi'^2} = (\beta - q)^2 \overline{\left(\frac{u'}{u}\right)^2}_{\omega} + \alpha^2 \left( \overline{\left(\frac{T'_\infty}{\overline{T}_\infty}\right)^2}_{sn} + \overline{\left(\frac{T'_\infty}{\overline{T}_\infty}\right)^2}_{\sigma} \right) +$$

$$(q - \beta)^2 \frac{1}{\gamma^2 M^4} \overline{\left(\frac{p'}{p}\right)^2}_{sn} \cos^2\theta + \qquad \text{B-18}$$

$$2\alpha(q - \beta) \frac{1}{\gamma M^2} R_{pT_\infty} \left(\frac{\tilde{T}_\infty}{\overline{T}_\infty}\right)_{sn} \left(\frac{\tilde{p}}{p}\right)_{sn}$$

If q = 0:

$$\overline{\phi'^2} = \beta^2 \overline{\left(\frac{u'}{u}\right)^2_\omega} + (s+\alpha)^2 \left( \overline{\left(\frac{T'_\infty}{T_\infty}\right)^2_{sn}} + \overline{\left(\frac{T'_\infty}{T_\infty}\right)^2_\sigma} \right) +$$

$$\beta^2 \frac{1}{\gamma^2 M^4} \overline{\left(\frac{p'}{p}\right)^2_{sn}} \cos^2\theta - \qquad \text{B-19}$$

$$2\beta(s+\alpha) \frac{1}{\gamma M^2} R_{pT_\infty} \left(\frac{\tilde{T}_\infty}{T_\infty}\right)_{sn} \left(\frac{\tilde{p}}{p}\right)_{sn}$$

Next consider the coexistence of vorticity and entropy. Equations A-2, A-4, and B-1 give:

$$\frac{e'}{E} = (\beta S_{T_o} - S_u)\left(\frac{u'}{u}\right)_\omega + (S_\rho + \alpha S_{T_o})\left(\frac{T'_\infty}{T_\infty}\right)_\sigma \qquad \text{B-20}$$

Squaring equation B-20, forming the mean, and dividing by $S^2_{T_o}$ gives:

$$\overline{\phi'^2} = (\beta - q)^2 \overline{\left(\frac{u'}{u}\right)^2_\omega} + (s+\alpha)^2 \overline{\left(\frac{T'_\infty}{T_\infty}\right)^2_\sigma} +$$

$$2(\beta - q)(s+\alpha) R_{uT_\infty} \left(\frac{\tilde{u}}{u}\right)_\omega \left(\frac{\tilde{T}'_\infty}{T_\infty}\right)_\sigma \qquad \text{B-21}$$

Equation B-18 shows that the fluctuation diagram for the combined effects of vorticity and entropy lies on a surface in the $\phi$, q, s coordinate system. The intersection of the surface with the q-plane can be found by letting s = 0. This gives:

$$\overline{\phi'^2} = (\beta - q)^2 \overline{\left(\frac{u'}{u}\right)^2}_{\omega} + \alpha^2 \overline{\left(\frac{T_\infty}{T_\infty}\right)^2}_{\sigma} +$$

$$2\alpha(\beta - q) R_{uT_\infty} \left(\frac{\tilde{u}}{u}\right)_{\omega} \left(\frac{\tilde{T}'_\infty}{T_\infty}\right)_{\sigma} \qquad \text{B-22}$$

If q = 0, the intersection of the surface with the $\phi$-s plane is given by:

$$\overline{\phi'^2} = \beta^2 \overline{\left(\frac{u'}{u}\right)^2}_{\omega} + (s + \alpha)^2 \overline{\left(\frac{T_\infty}{T_\infty}\right)^2}_{\sigma} +$$

$$2\beta(s + \alpha) R_{uT_\infty} \left(\frac{\tilde{u}}{u}\right)_{\omega} \left(\frac{\tilde{T}'_\infty}{T_\infty}\right)_{\sigma} \qquad \text{B-23}$$

Finally, consider the combined effects of vorticity and near-field sound. For these combined fluctuations, equations A-2, A-8 and B-1 gives:

$$\frac{e'}{E} = (\beta S_{T_o} - S_u)\left(\frac{u'}{u}\right)_{\omega} + (S_\rho + \alpha S_{T_o})\left(\frac{T'_\infty}{T_\infty}\right)_{sn} +$$

$$(S_u \cos\theta - S_\rho \gamma M^2 - \beta S_{T_o} \cos\theta)\frac{1}{\gamma M^2}\left(\frac{p'}{p}\right)_{sn} \qquad \text{B-24}$$

Squaring equation B-17, forming the mean, and dividing by $S_{T_o}^2$ and assuming that there is no correlation between vorticity and sound gives:

$$\overline{\phi'^2} = (\beta - q)^2 \overline{\left(\frac{u'}{u}\right)^2_\omega} + \qquad \text{B-25}$$

$$(q - \beta)\cos\theta - \gamma M^2 s]^2 \frac{1}{\gamma^2 M^4} \overline{\left(\frac{p'}{p}\right)^2_{sn}} + (s + \alpha)^2 \overline{\left(\frac{T'_\infty}{T_\infty}\right)^2_{sn}} +$$

$$2(s + \alpha)[(q - \beta)\cos\theta - \gamma M^2 s] \frac{1}{\gamma M^2} R_{pT_\infty} \left(\frac{\tilde{p}}{p}\right)_{sn} \left(\frac{\tilde{T}_\infty}{T_\infty}\right)_{sn}$$

If s = 0 then:

$$\overline{\phi'^2} = (\beta - q)^2 \overline{\left(\frac{u'}{u}\right)^2} + [(q - \beta)\cos\theta]^2 \frac{1}{\gamma^2 M^2} \overline{\left(\frac{p'}{p}\right)^2_{sn}} +$$

$$\alpha^2 \overline{\left(\frac{T'_\infty}{T_\infty}\right)^2_{sn}} + 2\alpha[(q - \beta)\cos\theta] \frac{1}{\gamma M^2} R_{pT_\infty} \left(\frac{\tilde{p}}{p}\right)_{sn} \left(\frac{\tilde{T}_\infty}{T_\infty}\right)_{sn}$$

B-26

If q = 0:

$$\overline{\phi'^2} = \beta^2 \overline{\left(\frac{u'}{u}\right)^2_\omega} + [-\beta\cos\theta - \gamma M^2 s]^2 \frac{1}{\gamma^2 M^4} \overline{\left(\frac{p'}{p}\right)^2_{sn}} + \qquad \text{B-27}$$

$$(s+\alpha)^2 \overline{\left(\frac{T'_\infty}{T_\infty}\right)^2_{sn}} - 2(s+\alpha)[\beta\cos\theta + \gamma M^2 s] \frac{1}{\gamma M^2} R_{pT_\infty} \left(\frac{\tilde{p}}{p}\right)_{sn} \left(\frac{\tilde{T}_\infty}{T_\infty}\right)_{sn}$$

<Blank Page>

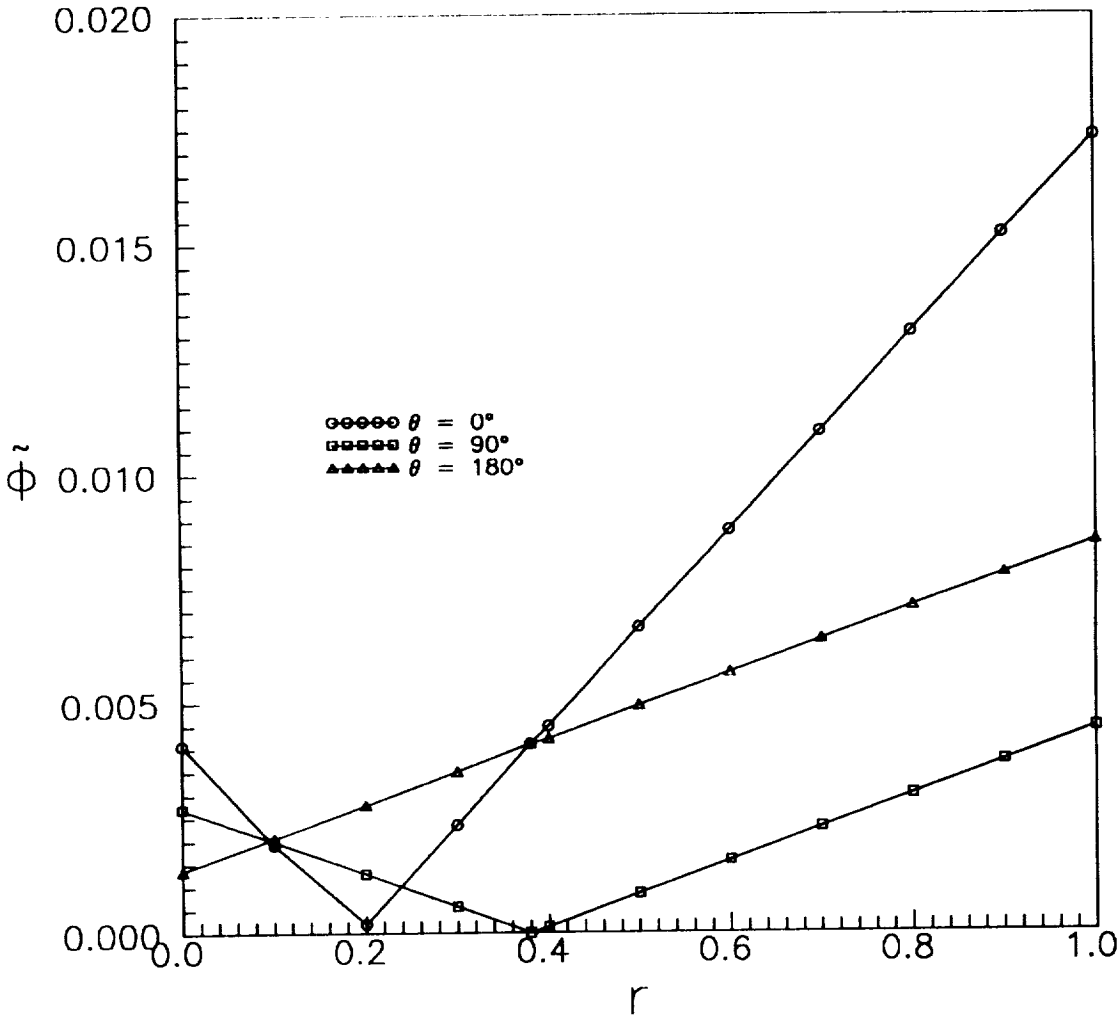


Figure 1. Far Field Sound mode
$S_u = S_\rho$; $(\tilde{p}/p)_{sf} = 0.01$; M=0.50

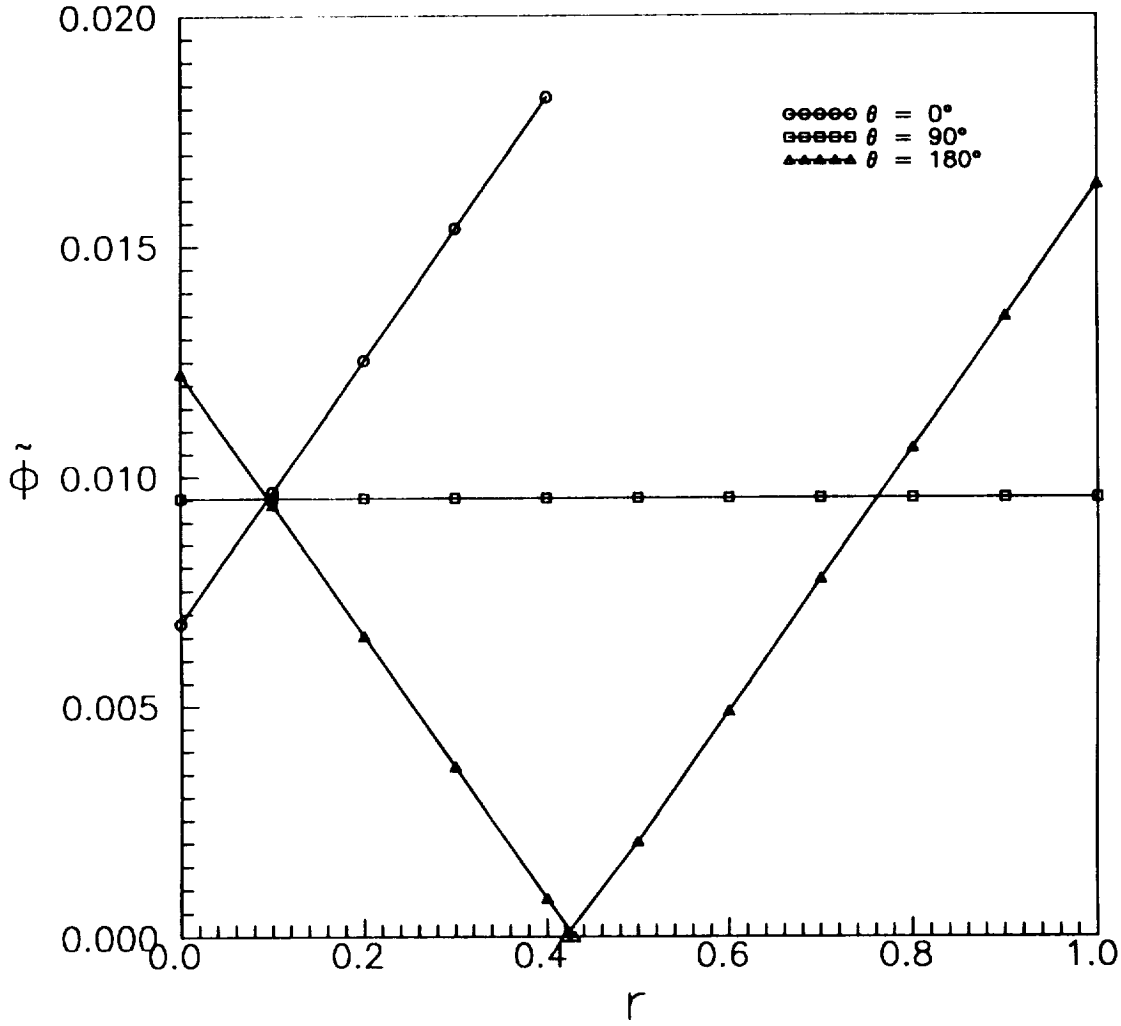


Figure 2. Near field sound fluctuation diagram;
$S_u = S_\rho$; $(\tilde{p}/p)_{sn} = 0.01$; $(\tilde{T}_\infty/T_\infty)_{sn} = 0.01$
$R_{pT_\infty} = 1.0$; $M = 0.50$

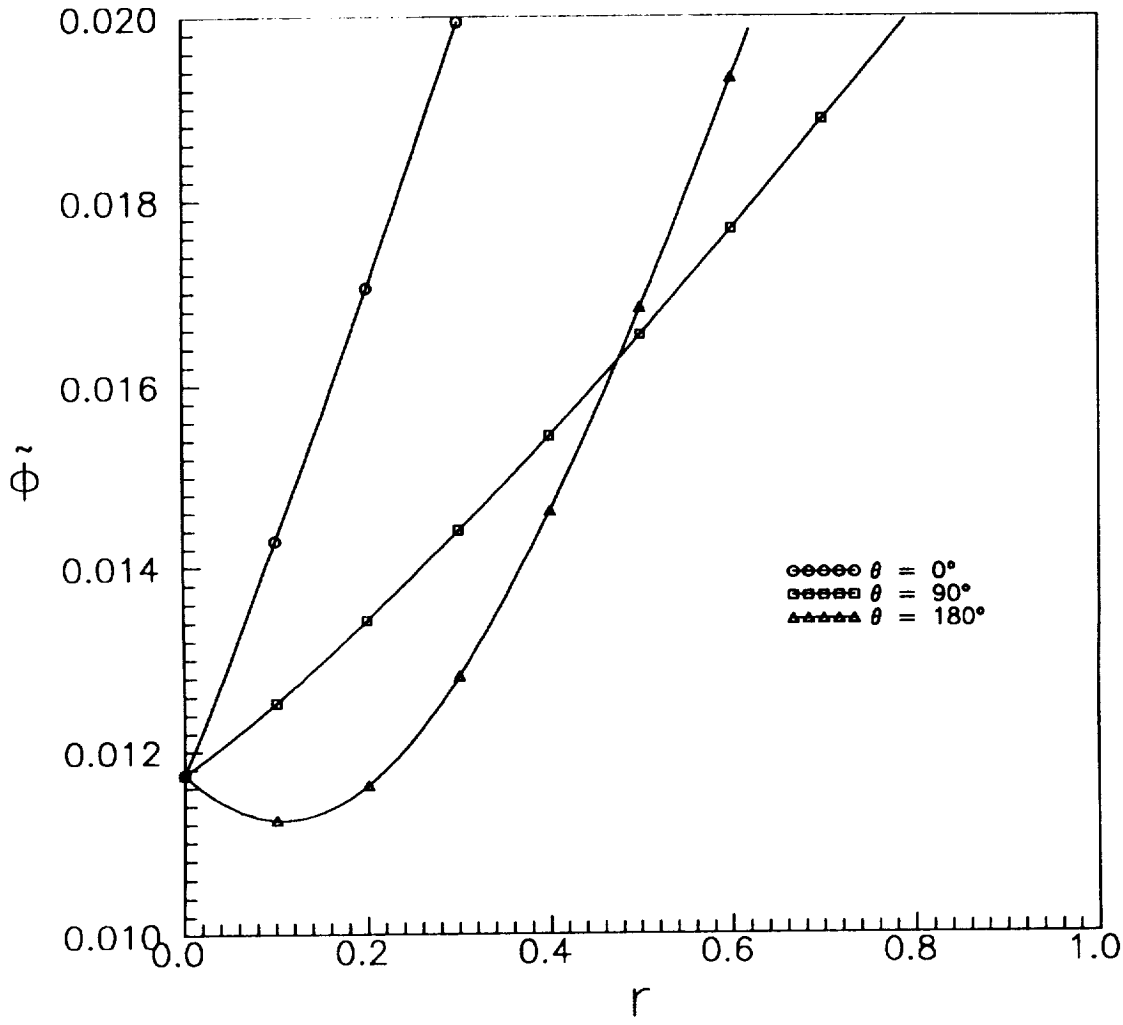


Figure 3. Fluctuation diagram for multi-mode fluctuations of vorticity, entropy and near field sound; $(\tilde{p}/p)_{sn} = 0.01$; $(\tilde{u}/u)_{\omega} = 0.01$; $(\tilde{T}_{\infty}/T_{\infty})_{sn} = 0.01$; $(\tilde{T}_{\infty}/T_{\infty})_{\sigma} = 0.01$; $R_{pT_{\infty}} = 1.00$; $M = 0.50$

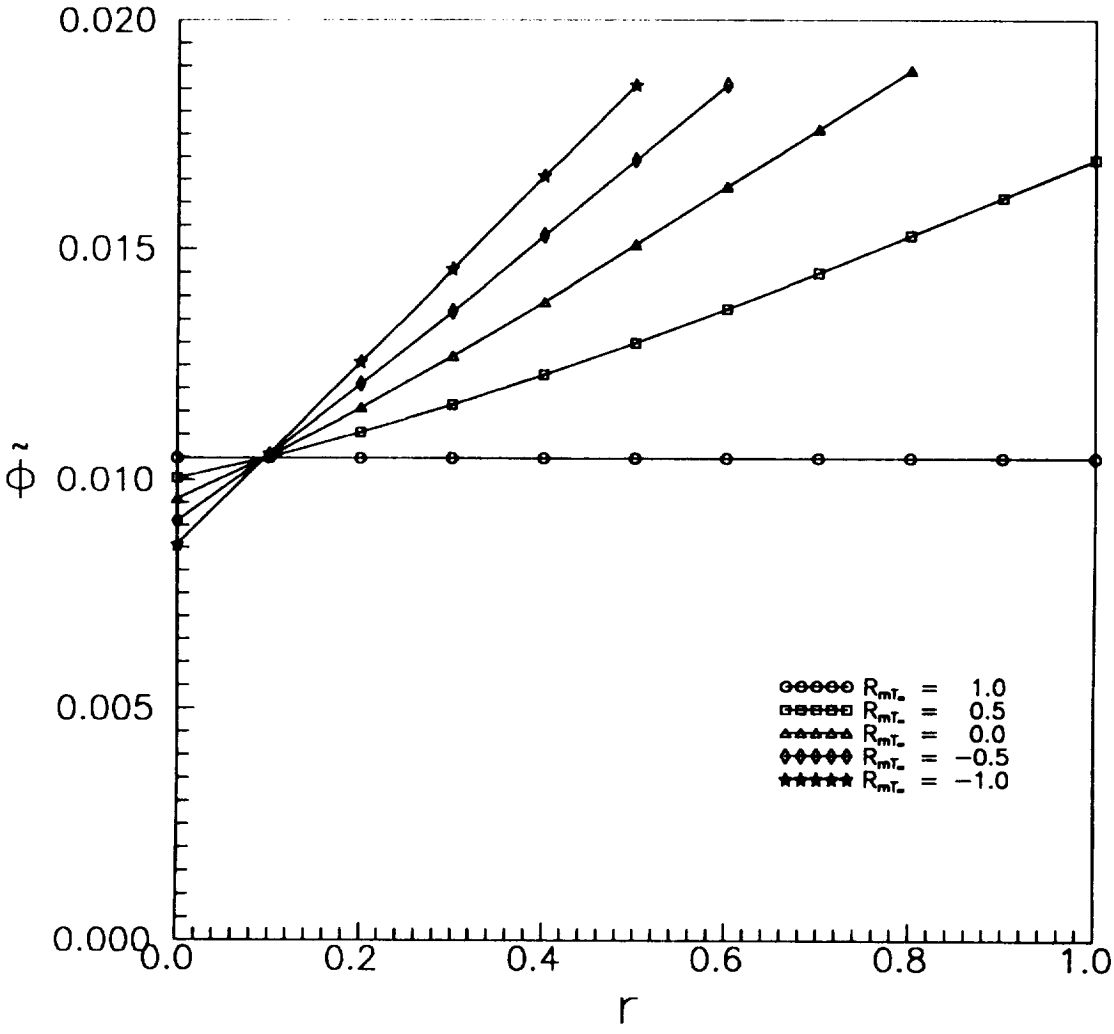


Figure 4. Fluctuation diagram for multi−mode fluctuations of vorticity and entropy; $S_u = S_\rho$ $(\tilde{u}/u)_\omega = 0.01$; $(\tilde{T}_\infty/T_\infty)_\sigma = 0.01$; $M = 0.50$

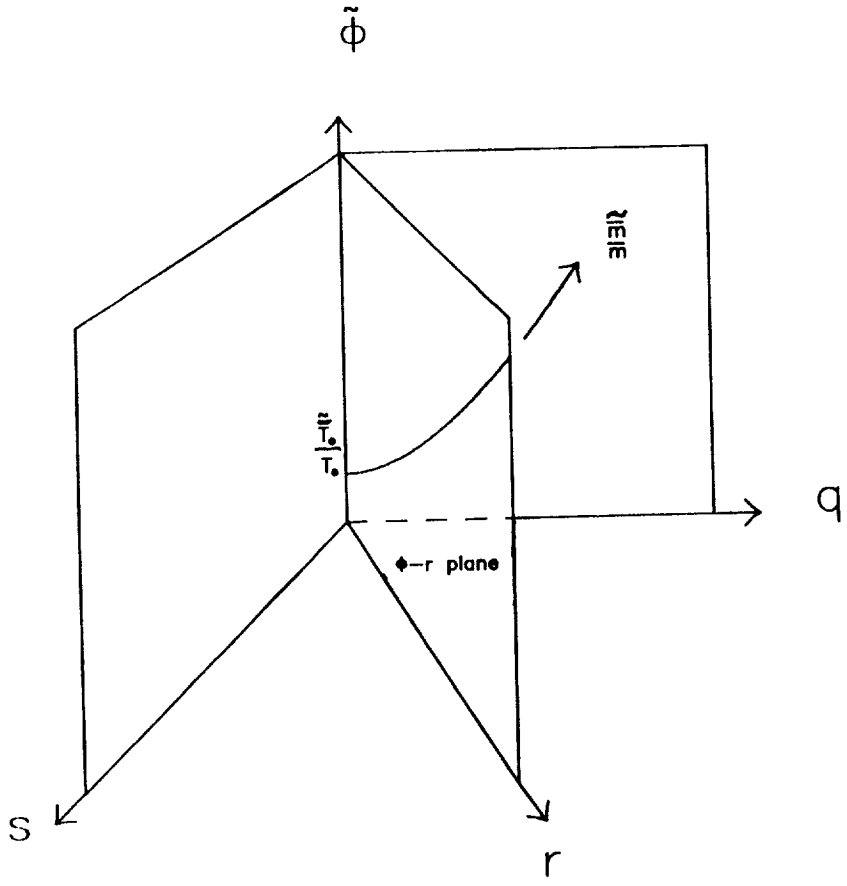


Figure 7. Fluctuation diagram for supersonic flow in the $\Phi$,q,s co–ordinate system; q = s

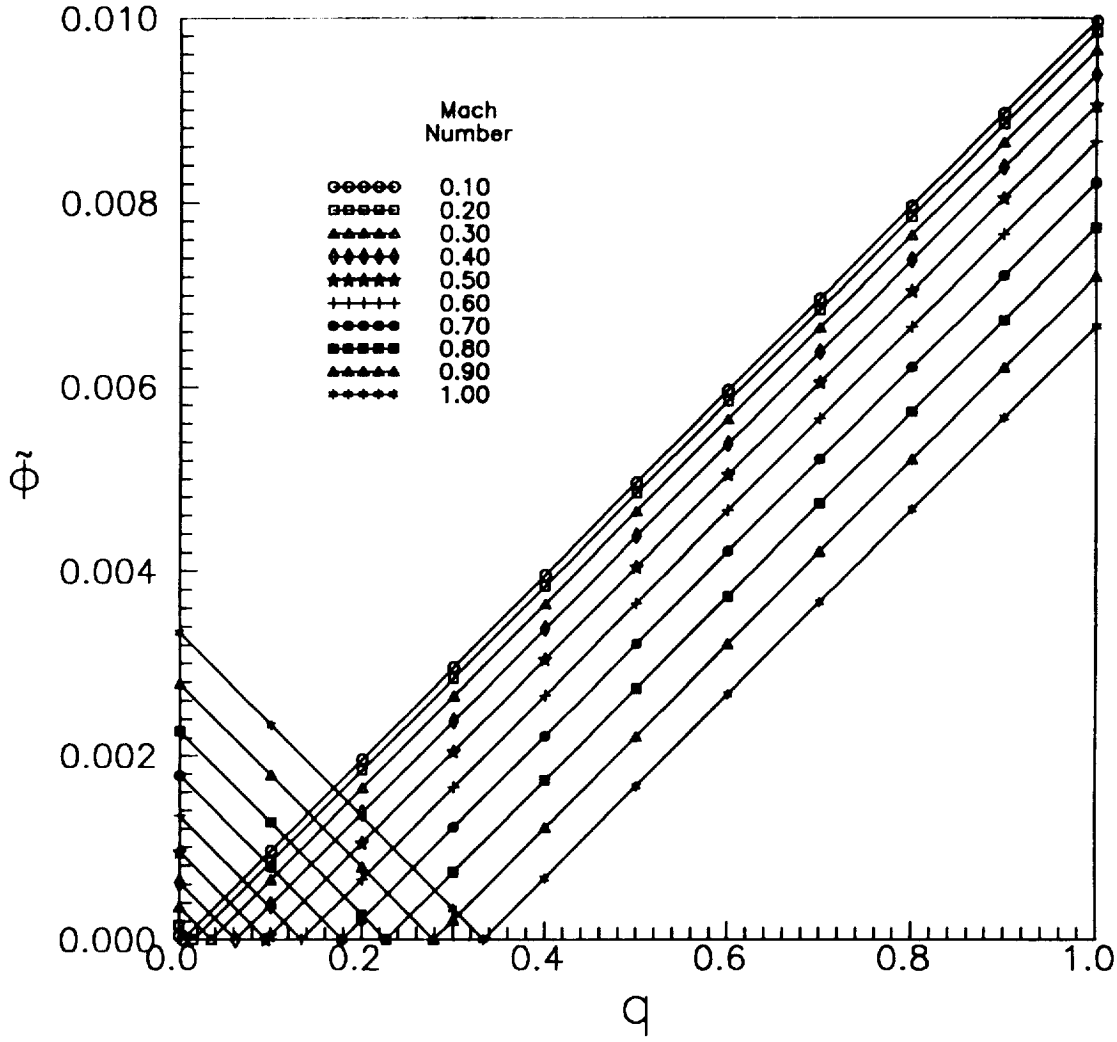


Figure 8. Vorticity Mode; $\tilde{u}/u = 0.01$

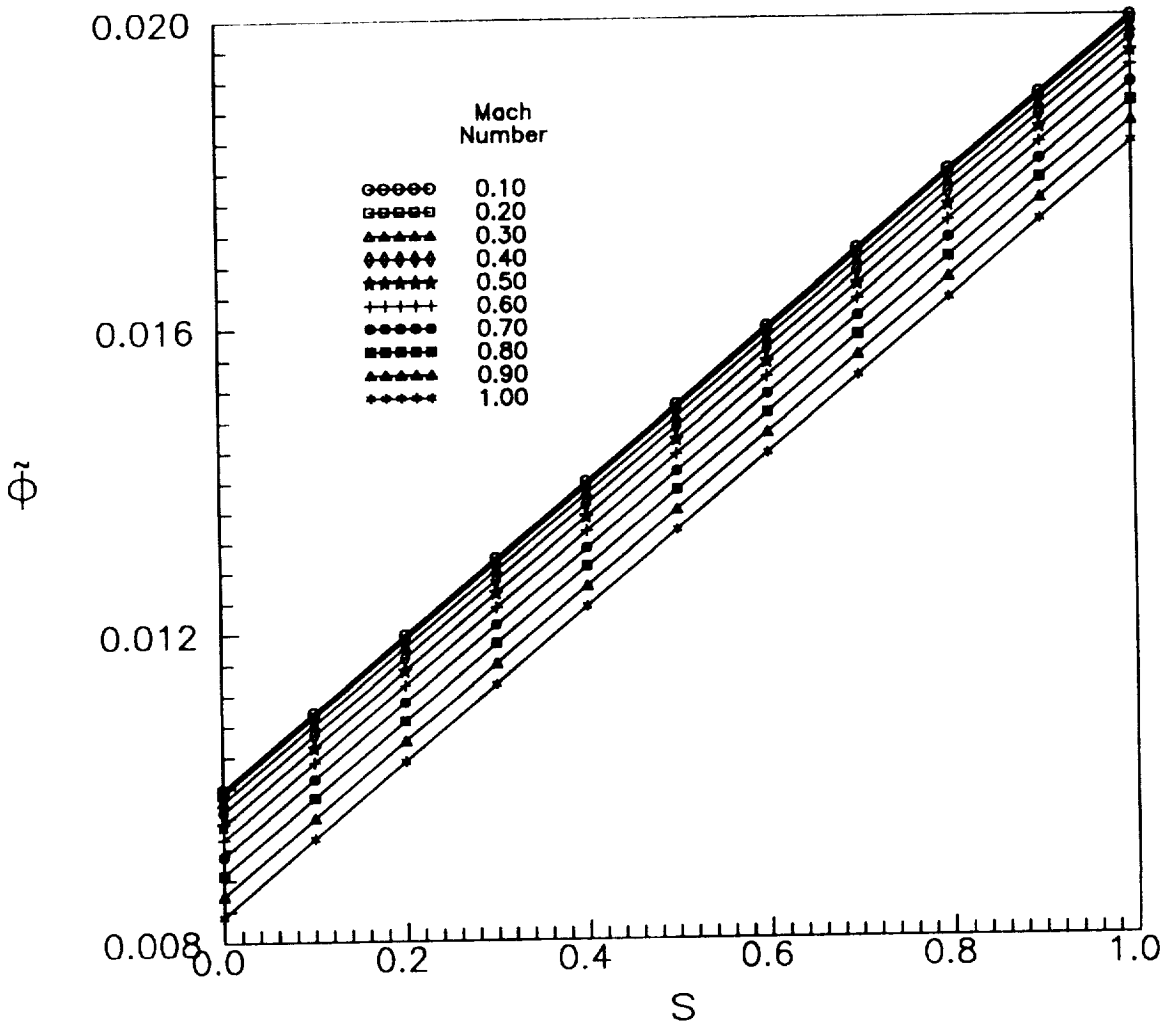


Figure 9. Entropy Mode; $\tilde{T}_\infty / T_\infty = 0.01$

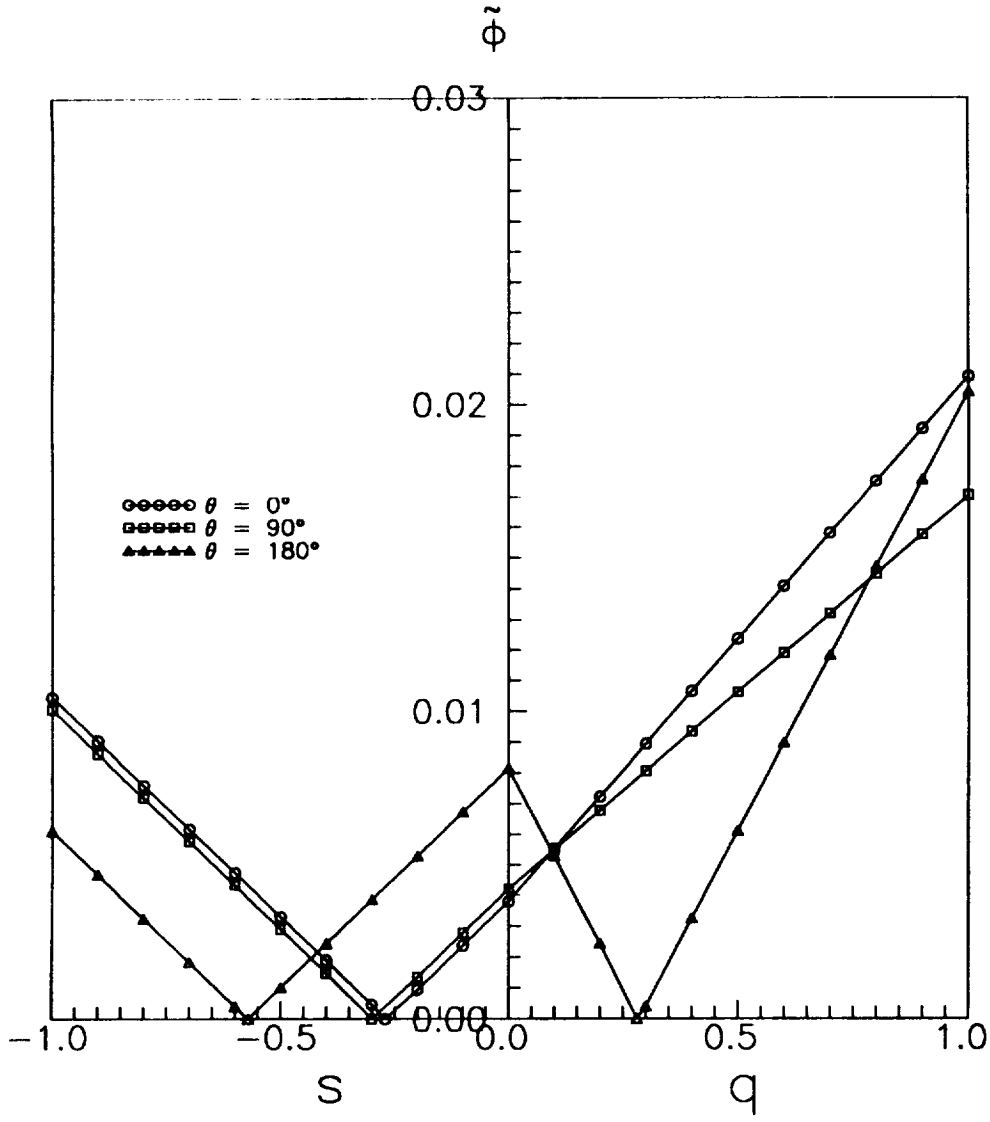


Figure 10. Far Field Sound Mode;
M = 0.50, $(\tilde{p}/p)_{sf}$ = 0.01, $S_u \neq S_\rho$

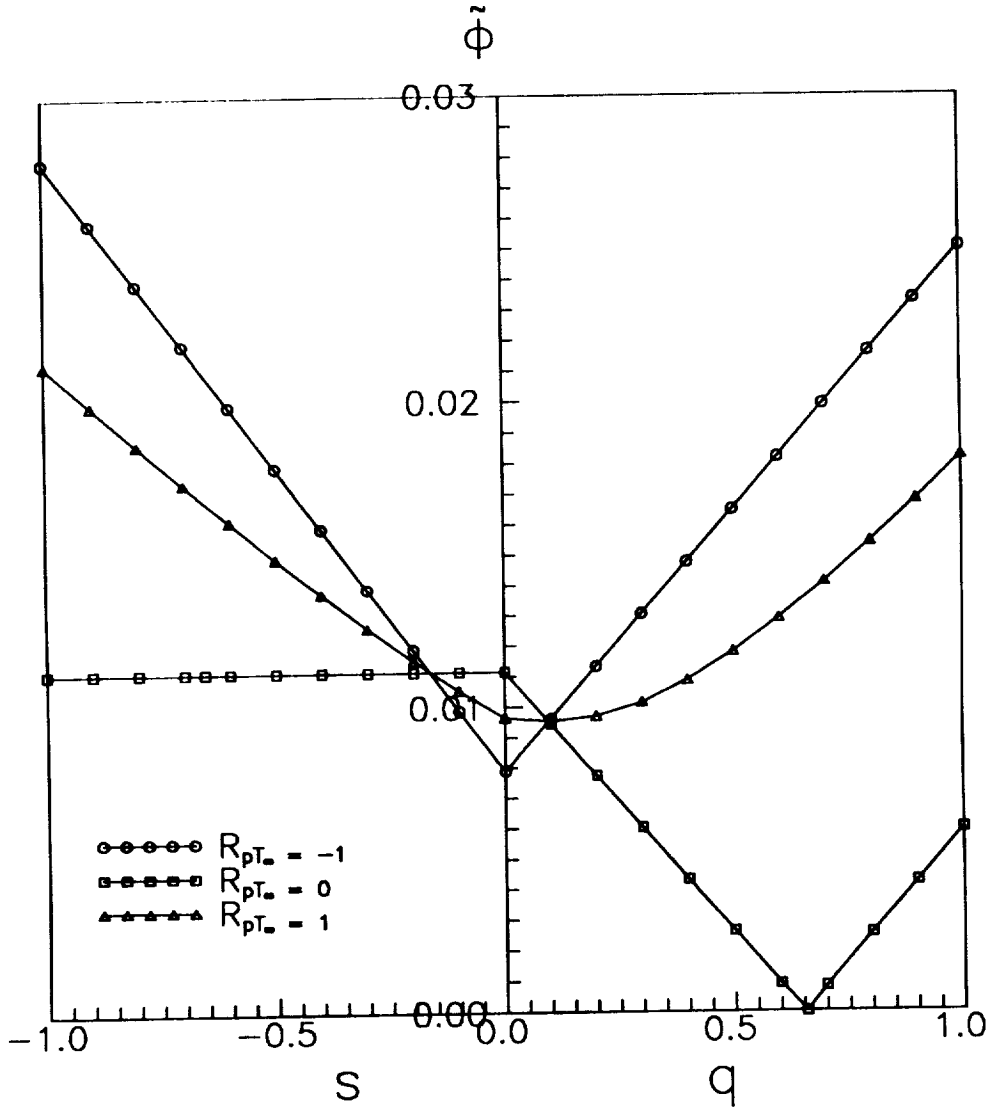


Figure 11. Fluctuation Diagram for Near Field Sound
$M = 0.50$, $\tilde{p}/p = 0.01$, $\tilde{T}_\infty/T_\infty = 0.01$,
$\theta = 180°$, $S_u \neq S_p$

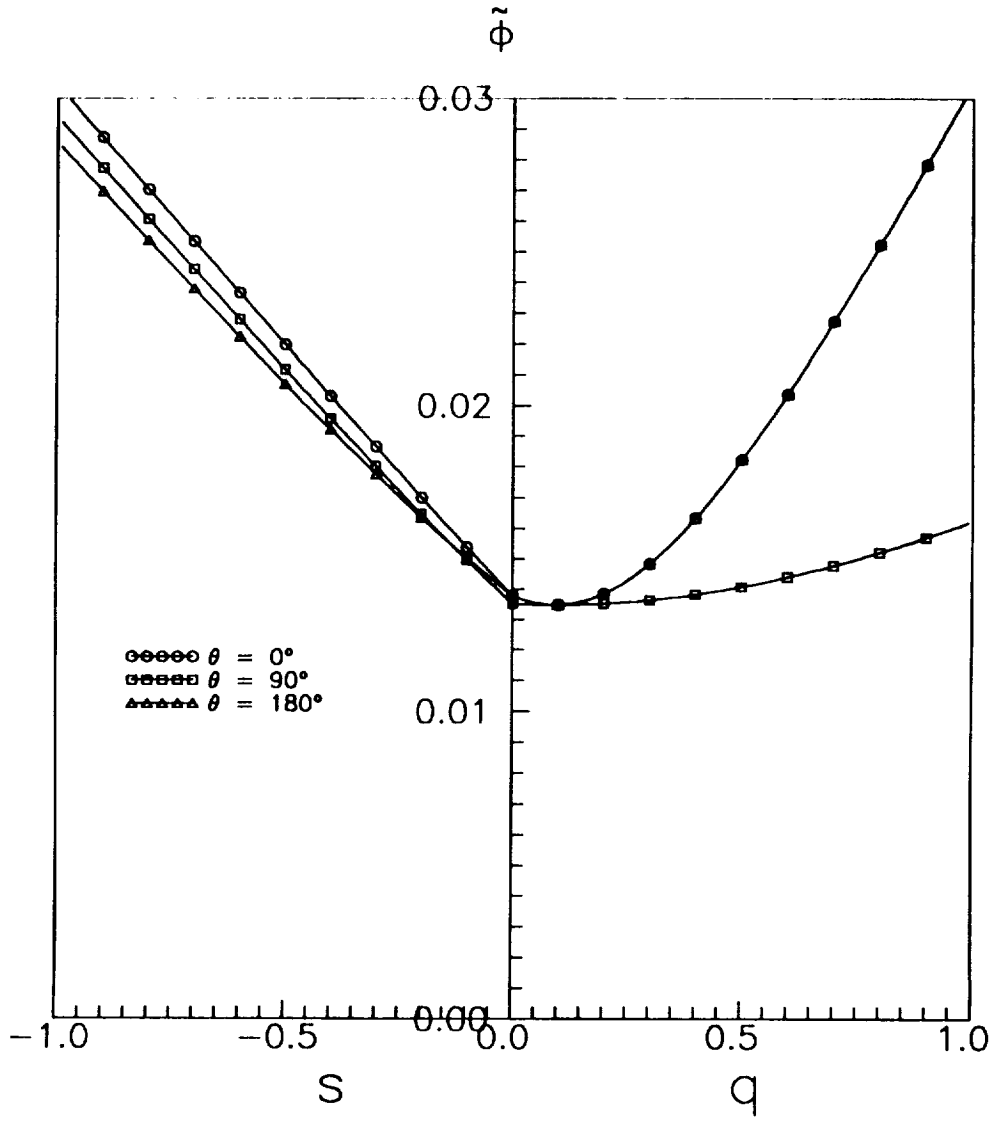


Figure 12. Fluctuation diagrams for vorticity, entropy and near field sound; $S_u \neq S_\rho$; $M = 0.50$; $R_{u(T_\infty)sn} = 0$; $R_{(T_\infty)_\sigma(T_\infty)sn} = 0$; $R_{u(T_\infty)_\sigma} = 0$; $(\tilde{p}/p)_{sn} = 0.01$; $(\tilde{u}/u)_\omega = 0.01$; $(\tilde{T}_\infty/T_\infty)_{sn} = 0.01$; $(\tilde{T}_\infty/T_\infty)_\rho = 0.01$

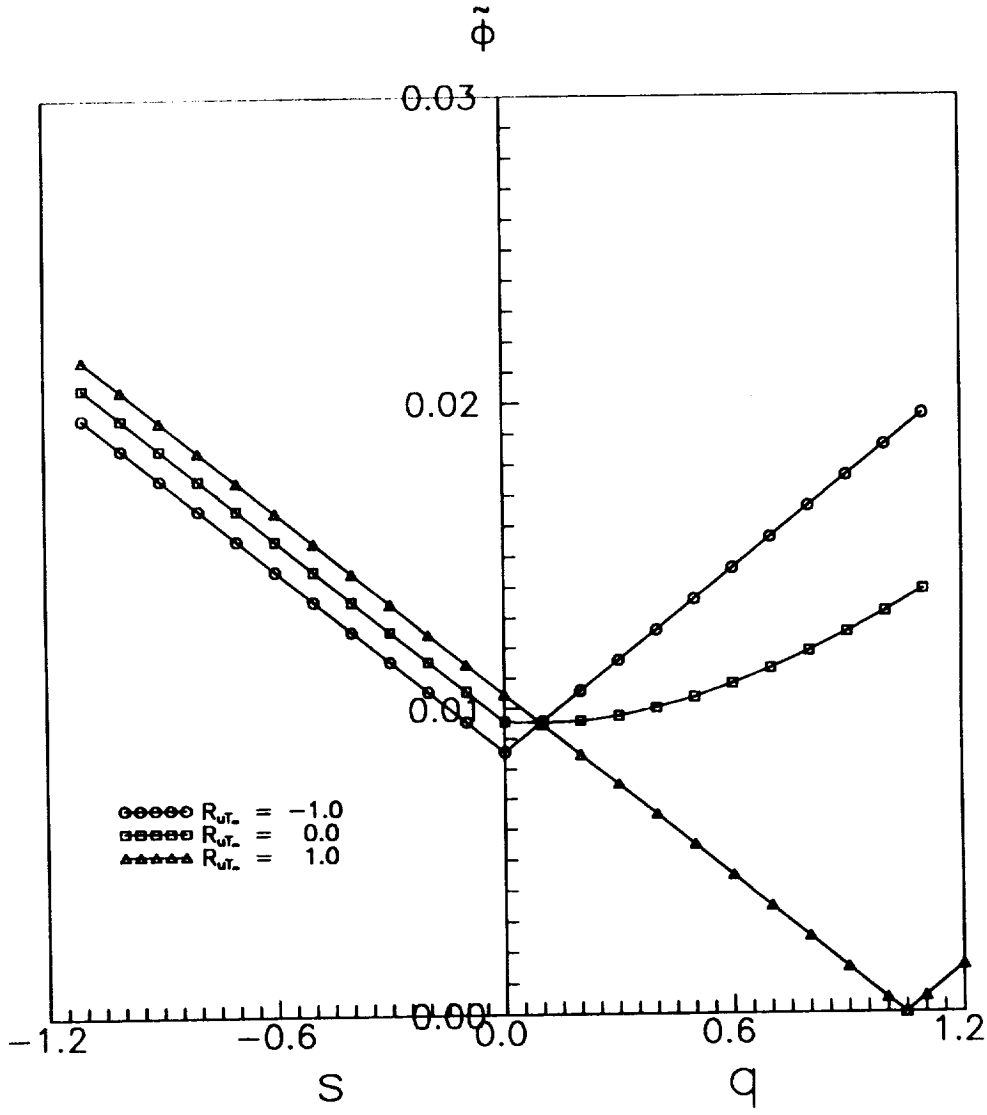


Figure 13. Fluctuation diagram for vorticity and entropy; $S_u \neq S_\rho$; $(\tilde{u}/u)_\omega = 0.01$; $(\tilde{T}/T)_\sigma = 0.01$; $M = 0.50$

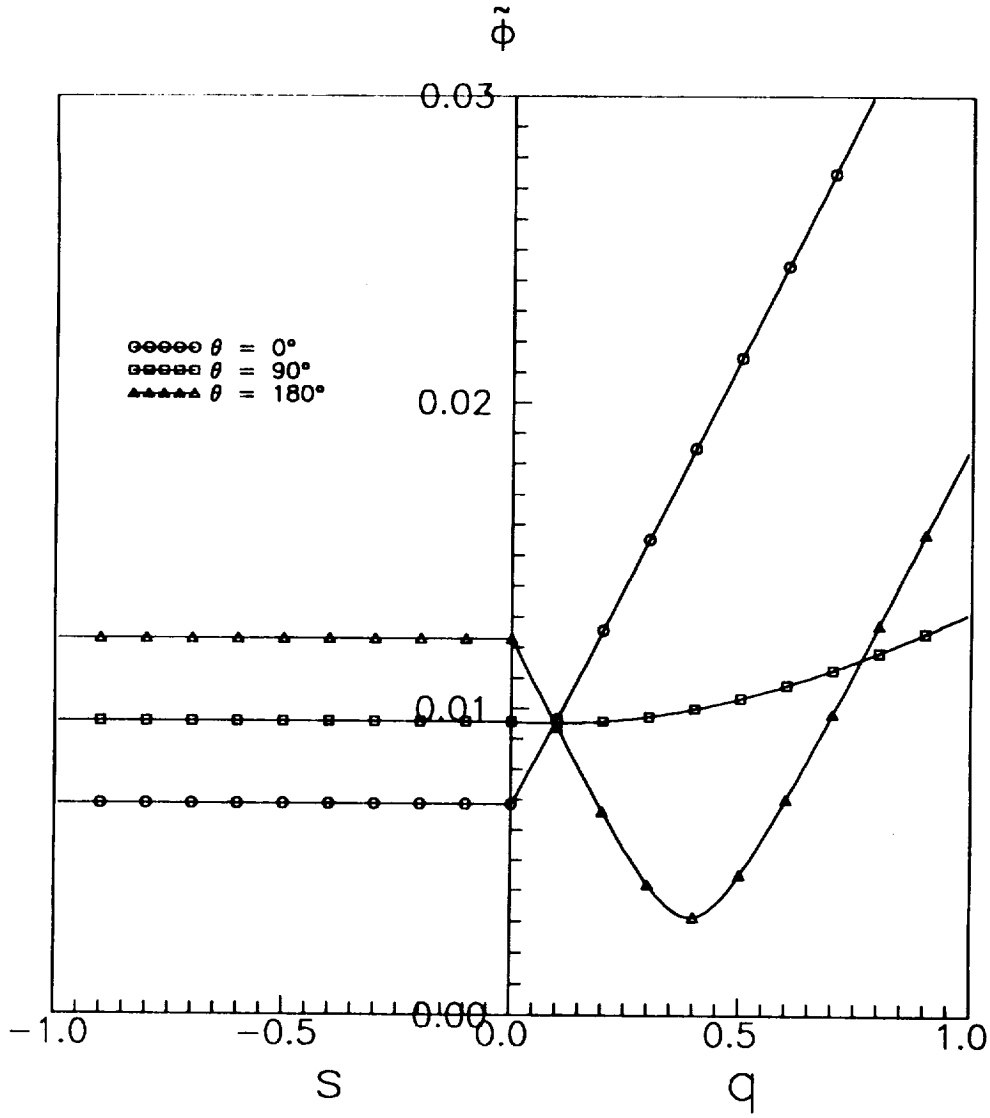


Figure 14. Fluctuation diagram for vorticity and near field sound; $S_u \neq S_\rho$; $R_{pT_\infty} = 1.00$; $M = 0.50$

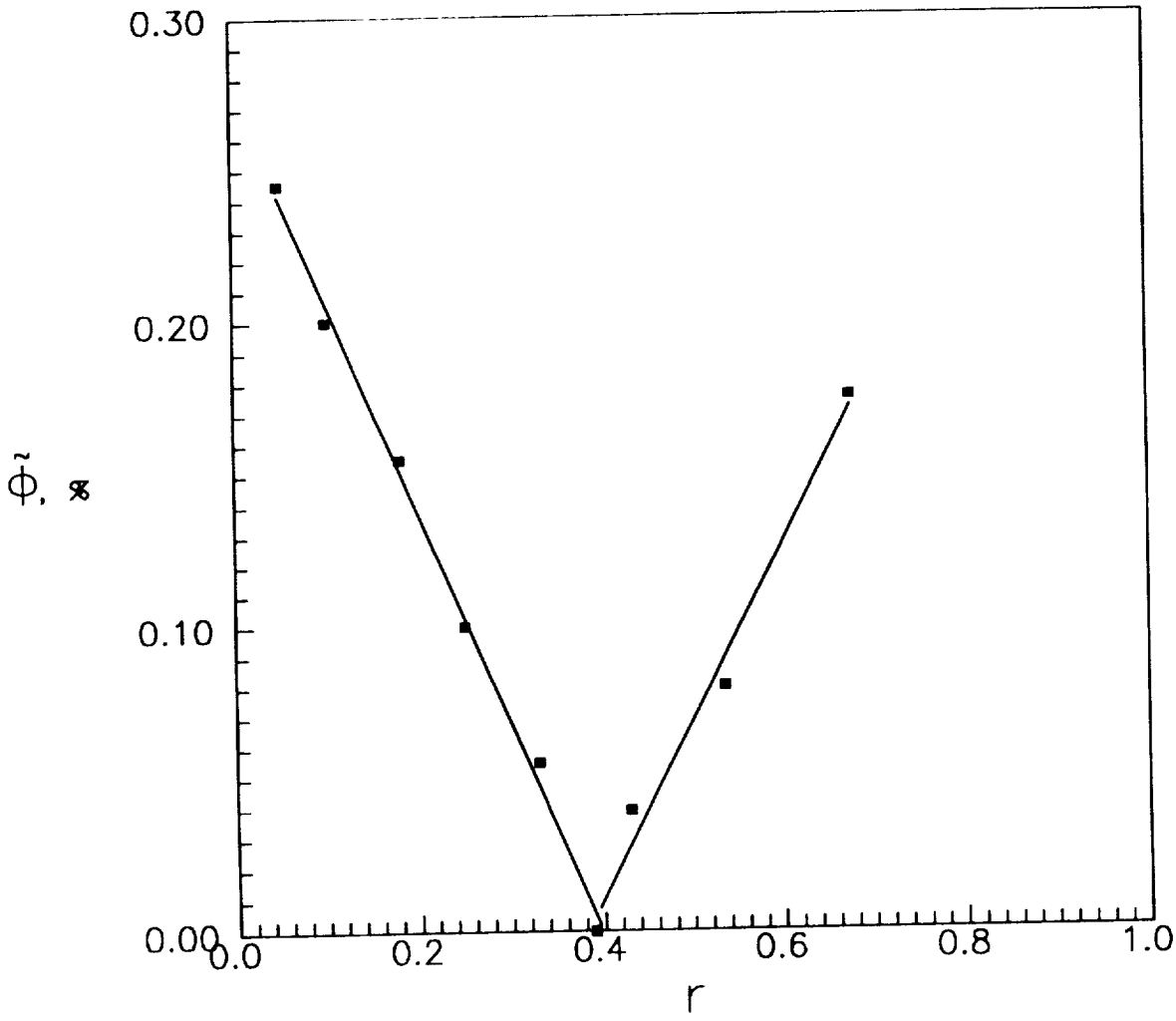


Figure 15. Measured Modes in Subsonic Flow, Ref. 3
(a) Far-Field Sound Modes; M = 0.72

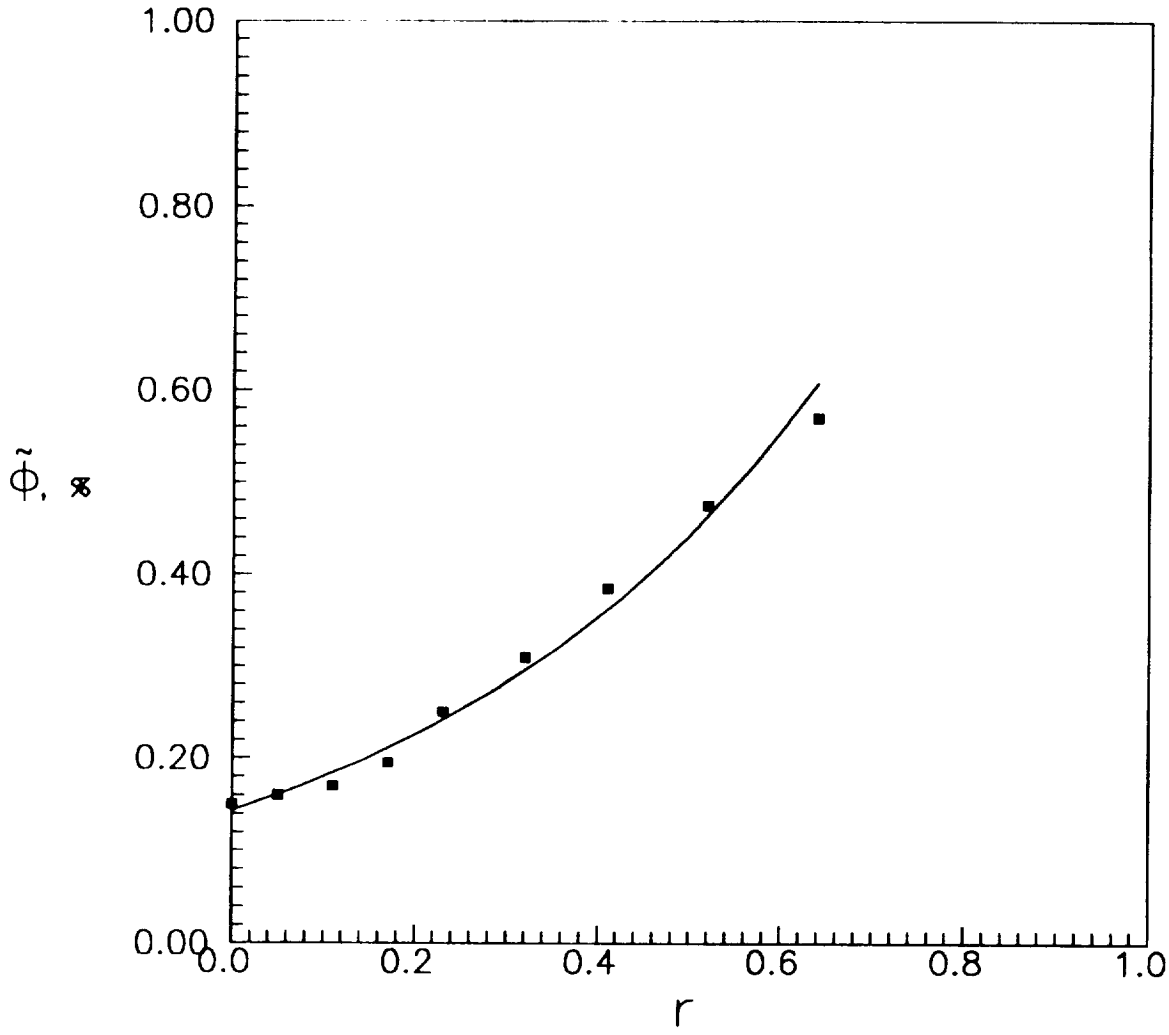


Figure 15. Measured Modes in Subsonic Flow, Ref.3
(b) Vorticity and Entropy Modes; M = 0.72

# REPORT DOCUMENTATION PAGE

Form Approved
OMB No. 0704-0188



**1. AGENCY USE ONLY** *(Leave blank)*

**2. REPORT DATE**
December 1991

**3. REPORT TYPE AND DATES COVERED**
Contractor Report

**4. TITLE AND SUBTITLE**
Fluctuation Diagrams for Hot-Wire Anemometry in Subsonic Compressible Flows

**5. FUNDING NUMBERS**
C NAS1-19320
C NAS1-18585
WU 505-59-50-02

**6. AUTHOR(S)**
P. C. Stainback
K. A. Nagabushana

**7. PERFORMING ORGANIZATION NAME(S) AND ADDRESS(ES)**
Analytical Services & Materials, Inc.
Hampton, VA 23666
and
Vigyan, Inc.
Hampton, VA 23666

**8. PERFORMING ORGANIZATION REPORT NUMBER**

**9. SPONSORING/MONITORING AGENCY NAME(S) AND ADDRESS(ES)**
NASA Langley Research Center
Hampton, VA 23665-5225

**10. SPONSORING/MONITORING AGENCY REPORT NUMBER**
NASA CR-189580

**11. SUPPLEMENTARY NOTES**
Langley Technical Monitor: Stephen P. Wilkinson

**12a. DISTRIBUTION/AVAILABILITY STATEMENT**
Unclassified - Unlimited

Subject Category 34

**12b. DISTRIBUTION CODE**

**13. ABSTRACT** *(Maximum 200 words)*

The concept of using "fluctuation diagrams" for describing basic fluctuations in compressible flows was reported by Kovasznay in the 1950's. The application of this technique, for the most part, was restricted to supersonic flows. Recently, Zinov'ev and Lebiga published reports where they considered the fluctuation diagrams in subsonic compressible flows. For the above studies, the velocity and density sensitivities of the heated wires were equal. However, there are considerable data, much taken in the 1950's, which indicate that under some conditions the velocity and density sensitivities are not equal in subsonic compressible flows. Therefore, the present report will describe possible fluctuation diagrams for the cases where the velocity and density sensitivities are equal and the more general case where they are unequal.

**14. SUBJECT TERMS**
Hot-Wire Technique
Fluctuating Diagram
Mode Diagram
Compressible Subsonic Flow
Heat Transfer
Sensitivity

**15. NUMBER OF PAGES**
57

**16. PRICE CODE**
A04

| 17. SECURITY CLASSIFICATION OF REPORT | 18. SECURITY CLASSIFICATION OF THIS PAGE | 19. SECURITY CLASSIFICATION OF ABSTRACT | 20. LIMITATION OF ABSTRACT |
|---|---|---|---|
| Unclassified | Unclassified | | |